Strain-rate and temperature dependent material properties of Agar and Gellan Gum used in biomedical applications

STRAIN-RATE AND TEMPERATURE DEPENDENT MATERIAL PROPERTIES OF AGAR AND GELLAN GUM USED IN BIOMEDICAL APPLICATIONS

Alessandro Schiavi[a]*, **Rugiada Cuccaro**[a], **Adriano Troia**[a]
[a] *INRiM – Istituto Nazionale di Ricerca Metrologica, Strada delle Cacce 91,10135 Torino, Italy*

* Corresponding author. Tel: +39 0113919916, Fax: +39 0113919621
E-mail addresses: a.schiavi@inrim.it (A. Schiavi), r.cuccaro@inrim.it (R. Cuccaro), a.troia@inrim.it (A. Troia)

Abstract

Agar and Gellan Gum are biocompatible polymers extensively used in several fields of tissue engineering research (e.g. tissue replacement, tissue support, tissue mimicking), due to their mechanical behaviour effectively representative of actual biological tissues. Since mechanical properties of artificial tissues are related to biocompatibility and functionality of medical implants and significantly influence adhesion, growth and differentiation of cells in tissue-engineering scaffolds, an accurate characterization of Young's modulus and relaxation time processes is needed. In this study, the strain-rate and temperature dependent material properties of Agarose and one among the numerous kind of Gellan Gum commercially available, known as Phytagel®, have been investigated.

Nine hydrogel samples have been realized with different mechanical properties: the first one Agar-based as a reference material, the further eight samples Gellan Gum based in which the effect of dispersed solid particles like kieselguhr and SiC, as enhancing mechanical properties factors, have been investigated as a function of concentration.

Stress-strain has been investigated in compression and relaxation time has been evaluated by means of the Kohlrausch-Williams-Watts time decay function. Mechanical properties have been measured as a function of temperature between 20 °C and 35 °C and at different strain rates, from ~10^{-4} s^{-1}

and ~10^{-3} s^{-1} (or deformation rate from ~ 0.01 mm·s^{-1} to ~ 0.1 mm·s^{-1}). From experimental data, the combined temperature and strain-rate dependence of hydrogels Young's modulus is determined on the basis of a constitutive model.

In addition to a dependence of Young's modulus on temperature, a remarkable influence of strain-rate has been observed, especially in the sample containing solid particles; in same ranges of temperature and strain-rate, also relaxation time variations have been monitored in order to identify a possible dependence of damping properties on temperature and strain-rate. The result is the impossibility to determine univocally mechanical properties of studied biomaterials without a proper definition of boundary conditions at which they have been obtained.

Keywords
Hydrogels, Young's modulus, relaxation time, temperature-dependence, strain-rate-dependence.

1 Introduction

In the field of tissue engineering and regenerative medicine, tunable mechanical properties for optimizing tissue regeneration *in vivo* and tissue formation *in vitro* are recognized as a fundamental requirement for biomaterials. Hydrogels, in general terms, give opportunity to easily develop mimic tissues with tunable mechanical properties over a wide range of stiffness [1], in particular to simulate soft biological materials (100 kPa < E < 1 GPa) [2] and ultra-soft biological materials (E < 100 kPa) [3, 4]. As well as biochemical properties, mechanical properties of hydrogels influence many different biological features such as biocompatibility and functionality of medical implants and tissue-engineering scaffolds [5 – 7], and to degradable biocompatibility of organ-based tissue engineering implants [8]. Moreover, as recently debated, mechanical properties and microstructure of scaffolds seem to influence cell behaviour and overall scaffold bioactivity. Recent experiments

have revealed that stem cells respond to biophysical cues as well as numerous biochemical factors. In the heterogeneous microenvironments referred to as stem cell niches, various mechanical (united with biomolecular) cues are integrated to maintain pluripotency or to induce differentiation [9].

On the other hand, due to their significant similarity to actual human tissues, hydrogels are also extensively used in laboratory tests. For instance, they are used as versatile platform in the study of cell-substrate interactions as well as tissue-mimicking materials (TMMs) in the investigation of mechanical and thermal effects in tissues due to ultrasounds [10 -12]. As a consequence, a proper characterization of the mechanical properties of these materials allows to evaluate with higher accuracy technical performances, biological behaviours or other related phenomena associated with them.

In this work samples of TMMs, Agarose and Phytagel® based, have been opportunely realized with different concentration of Kieselghur and SiC in order to evaluate the effects on the mechanical behaviour as a function of temperature and strain-rate. TMMs here investigated only simulate soft biological materials in the range between 100 kPa and 1 MPa. Their similarity to soft biological tissues from the attenuation and speed of sound point of view has been previously investigated and some of the results have been published in [28].

The mechanical behaviour of hydrogels is evaluated on the basis of the theories of rubber elasticity and viscoelasticity [13]. Despite during the last decades mechanical properties of hydrogels have been deeply investigated by means of static, quasi-static and dynamic techniques and the elastic moduli have been determined in compression, extension, torsion, from resonance method and from micro- and nano-indentation, less known are the mechanical properties of hydrogel as a function of temperature and strain-rate. Temperature fluctuation and different speed of applied force induce relevant variations in elastic properties of hydrogels. As a matter of fact, relevant strain-rate dependences in actual human tissues properties have been observed [14-16].

Since environmental conditions, experimental procedures and measurement methods can affect experimental results, in this work the Young's modulus, E, and the relaxation time, , of nine hydrogel samples have been evaluated as a function of temperature (20 °C < T < 35 °C) at different very low strain-rates ($0.06 \cdot 10^{-2}$ s^{-1} < $\dot{\varepsilon}$ < $0.4 \cdot 10^{-2}$ s^{-1}) with the aim to achieve an effective characterization of the mechanical behaviour of biomaterials under investigation. In the considered ranges of temperature and strain-rate, a constitutive model to evaluate the average variability of Young's modulus, i.e. $E(T, \dot{\varepsilon})$, is then proposed.

Measurements have been carried out in unconfined compression. Yield and tensile strengths have been previously determined for each sample in standard laboratory conditions. On twin samples, within the elastic region, the effects of temperature and strain rate on Young's modulus and relaxation time have been determined.

2 Materials and experimental methods

2.1 Preparation of tissue mimicking materials

Hydrogel, in particular polysaccharides, as tissue-mimicking materials have been widely studied over last ten years. Nevertheless, the natural origin of these molecules, their purity, the grade of refining and the catalyst used for polymerization, when present, lead the researchers to obtain gel with notable differences in terms of mechanical properties, so that their use as tissue mimicking materials could be tuned for a wide class of biological tissues.

In our study we have investigated two types of polysaccharides: Agar and Gellan Gum. Agar is a well-known polysaccharide formed principally by Agarose [1]. It is insoluble in room temperature water, while it dissolves in boiling water, forming a gel when cooled down to a temperature of about 30-40 °C. This value depends on purity, on Agar concentration and pH. It has been largely studied from a mechanical and thermal point of view [17], it is used as phantom material for ultrasound imaging and hyperthermia applications [18], it is recommended as reference material for

flow Doppler test by the European standard IEC 61685 [19] and, in addition, it is commonly used as cell culture scaffold [20]. Moreover, its stiffness can be altered allowing for tuning scaffold mechanical properties. For these reasons, in this work it has been chosen to investigate, as first, a gel made of Agar. The sample has been prepared heating on a hot plate an aqueous solution of Agar (3% in weight) at 100 °C. Maintaining the solution under stirring, Benzalkonium chloride (0.9% in weight) as anti-fungal agent has been added. Successively, while the sample cooled, it has been cast carefully into a cylindrical mould to avoid bubbles formation and obtain very smooth and flat surfaces, fundamental to exercise an homogeneous force distribution, important aspect for the Young's modulus measurements.

Gellan Gum is a more complex polysaccharide. During last five years, this product have received more attention because of its higher temperature stability, higher mechanical strength and better clarity than Agar, besides a substantially lower cost, which makes it an attractive polymer for the realization of TMM matrix. Furthermore, modifying its chemical structure, its properties can be tuned to be suitable for tissue engineering purposes [21]. Structurally it comprises a repeated tetrasaccharide unit of two -D glucose, one of -D glucuronate and one -L rhamnose and, commercially, it is available with different trade name like Gelrite®, Kelcogel® or Phytagel®, whose different name corresponds to the different grade of deacylation. The native state has high “acyl” grade, while low “acyl” is prepared via alkali treatment. High “acyl” Gellan Gum forms a gel upon cooling from 65 °C creating a soft flexible hydrogel, while low “acyl” Gellan Gum forms a gel upon cooling below 45 °C creating a rigid and brittle hydrogel. Gellan Gum, like Agar or other polysaccharides, forms a physical gel by undergoing from random coil to double helix transition upon heating and cooling treatment. Stiffer gel are formed if cations are present during the sol-gel transition. Particularly, monovalent cations, like Na or K, form an intermediate strength hydrogel through electrostatic interaction with carboxylate group [22], while divalent cations, like Mg or Ca,

form stronger gels by the aggregation of multiple helix. In our preparations, we have used Phytagel® (by Sigma-Aldrich company) which has low deacylation grade, so that an hard and brittle gel has been expected to be obtained [23].

We have developed a new synthesis procedure to obtain an hard and strong TMM using calcium sulphate as catalyst and Potassium Sorbate as antifungal. In detail, we have prepared a solution of Ca_2SO_4 dihydrate (0.5 % in weight) and of Potassium Sorbate (0.1% in weight); the solution has been gradually heated up to 90 °C while kept under stirring. During this step, Phytagel® powder (conc. of 2% in weight) has been added to the solution. The presence of salt prevents the formation of lumps, allowing to keep homogenous the solution during the heating step. Hence the solution is heated up to boiling for 2 min (temperature about 95-100 °C) and left cooling down to 80 °C. At this step, the solution is rapidly poured into a cylindrical mould in order to minimize the inclusion of bubbles on the two surfaces, which should be very flat in order to exercise an homogeneous forces on the sample during the measurements. As it is reported in [24], the presence of calcium could affect the jellification temperature of Gellan Gum. To this end, we have observed a slight increase of the jellification temperature respect to temperatures (30 – 40 °C) reported in [24]. Investigated samples solidify very rapidly when in contact with mould cold surfaces, although the temperature of the solution is more than 60 °C. This characteristic has been exploited to minimize the settling of solid particles dispersed in TMM samples with the aim of enhancing their mechanical properties. Thus, we prepared different samples in which a specific amount of kieselguhr, a natural siliceous sedimentary powder with a particles dimension in range of 10 to 200 m, and/or Silicon Carbide (SiC) particles, with a mean dimension of 47 m, have been dispersed on Phytagel® matrix. Both this particles are considered biocompatible [25 - 27]. We added the particles during the heating step, when the solution reach 70 °C. The amount added to the solution varied from 0.5 up to 2% and from 0.75% up to 3% in weight respectively for SiC and kieselguhr. The whole preparation

set with respective ingredients is summarised in Table 1 and, hereafter, the name of each sample will correspond to the name given in the first column of the table.

	Agar	*Phytagel®*	*Ca_2SO_4*	*Kieselghur*	*SiC*	*Anti-fungal*
TMM 1	3	-	-	-	-	x
TMM 2	-	2	0.5	-	-	x
TMM 3	-	2	0.5	0.75	-	x
TMM 4	-	2	0.5	1.5	-	x
TMM 5	-	2	0.5	-	0.5	x
TMM 6	-	2	0.5	-	1	x
TMM 7	-	2	0.5	0.75	0.5	x
TMM 8	-	2	0.5	1.5	1	x
TMM 9	-	2	0.5	3	2	x

Table 1: Summury of investigated TMMs composition.. All reported values refer to in weight % concentration. Anti-fungal For TMM1 the anti-fungal agent is represented by Benzalkonium chloride (0.9% in weight), while for allother TMMs is given by Potassium Sorbate (0.1% in weight).

The choice of samples to study has been triggered by previous investigations of speed of sound and attenuation coefficient conducted on these materials [28]. Recently, several alternative TMMs have been proposed beyond the recipe reported in the European standard IEC 61685, since one of the key point is to obtain an homogeneous TMM with higher attenuation coefficient and enhanced mechanical properties.

2.2 Mechanical quantities measured

As many biological materials, TMMs investigated in this work show a viscoelastic behaviour. Performances of viscoelastic materials are affected by strain amplitude and strain-rate, by vibration frequency, static load and temperature.

At low strain rates, that means in standard compressive tests, heat generated by compression work is mainly dispersed in the environment, making the experiments to be considered about isothermal. On the contrary, at high strain-rates, the energy cannot be dispersed prior to material failure. The result is a localized increase in temperature in the damaged region and an adiabatic strain response

to applied stress. Since traumatic failures and lacerations *in vivo* [14, 15] have been related to the effects of strain-rate also for actual human tissues, an adequate characterization of TMMs mechanical behaviour as a function of the strain-rate could provide useful information for trauma mathematical models implementation or for the investigation of organ injury mechanisms.

The occurring variability of TMMs mechanical properties in a limited temperature range included between laboratory (20 °C) and human body (37 °C) temperature has been also quantified. Experimentally, Young's modulus values are determined from the ratio between the incremental stress and the incremental strain applying the classical Hooke's law at a constant strain rate, as shown below:

$$E = \frac{\Delta\sigma}{\Delta\varepsilon} = \frac{F}{A} \times \frac{l_0}{\Delta l}, \qquad (1)$$

where E is the Young's modulus (Pa), is the incremental stress (Pa), is the incremental strain (dimensionless), F is the compression force (N), A is the surface area of the sample (m^2) on which the force acts, l_0 is the initial thickness of the sample (m) and l is the deformation in thickness (m) resulting from the application of F within the region in which the sample under investigation shows an elastic behaviour. Plotting the incremental stress as a function of the strain, it is possible to determine the value of the sample elastic modulus by means of a linear fit.

Moreover, hydrogels viscoelastic behaviour can be evaluated from relaxation time processes after deformation, e.g. by means of the relation $\sigma(t) = E \times \varepsilon_0 (1 - \Phi(t))$, where ε_0 is the starting strain value and $\Phi(t)$ is the empirical Kohlrausch-Williams-Watts (KWW) time decay function. This function allows to obtain a more accurate interpolation of typical viscoelastic time decay than simple exponential Debye function. The KWW function is widely used to model several time-decaying behaviour of relaxation processes of viscoelastic materials and it is also used in polymers dynamics and in bone and muscle rheology [29]. KWW function is given by the following expression:

$$\Phi(t) = \exp\left(-\frac{t}{\tau_0}\right)^{\gamma}, \qquad (2)$$

where t is the time, τ_0 is the relaxation time at which $\Phi(t)$ decays to the value $1/e$ and the exponent γ describes the breadth of the distribution in the limits of $0 < \gamma \leq 1$. The distribution of relaxation times changes from a broad, symmetric distribution to a sharp, asymmetric one increasing γ from 0 to 1. The relaxation time is directly related to the material damping properties. In general terms, as τ_0 decreases, the internal damping tends to increase, and *vice versa*. As a result, a greater aptitude to dissipate or absorbing energy of mechanical stress occurs.

In the following, τ_0 and γ experimental data are analysed in order to highlight any possible influence of temperature and strain-rate over them.

In Figure 1, an example of a stress-strain and stress relaxation curve is shown. Red curve qualitatively represents the adopted measurement procedure from experimental data.

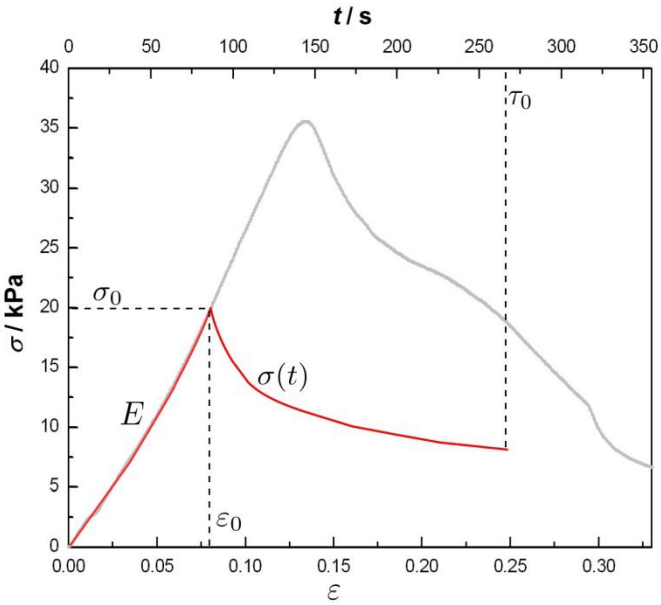

Figure 1: Stress-strain (grey) and stress relaxation (red) curve, with σ_0 and ε_0 respectively starting stress and strain values, E Young's modulus, t stress relaxation time, and τ_0 relaxation time at which $\Phi(t)$ decays to the value $1/e$.

2.3 Experimental apparatus and procedure

To measure the mechanical properties of TMMs, an uniaxial unconfined compression has been performed using a proper device specifically designed and realized at INRiM. Measurements have been carried out in displacement control and the resulting force has been measured downstream. The linear displacement has been performed by a stepping motor (Orientalmotor a-GRADE AR Series – AR HM 40093E 24DC) connected to a screw by means of a reduction gear. The displacement rates can be opportunely tuned from about 1 mm/s to 0.1 m/s. The linear displacement has been measured by means of a linear encoder Solartron LE25/S with an accuracy of 1 m (resolution 0.1 m). The resulting forces have been measured by means of a load cell HBM type Z3H3R, with a resolution of 5 mN. The evaluated uncertainty of the force, in the range between 10 N and 1000 N, can be considered lesser than ≤ 1‰. Calibration of the linear encoder and of the load cell have been performed at INRiM on the basis of the international standard calibration [30, 31] fulfilling proper metrological requirements. Figure 2 shows the experimental apparatus.

(a) 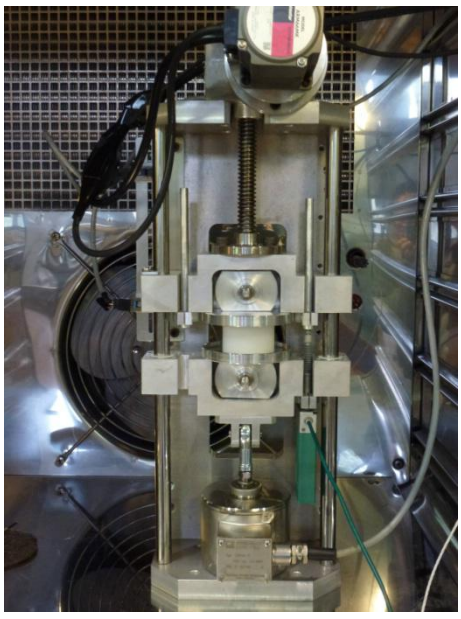 (b) 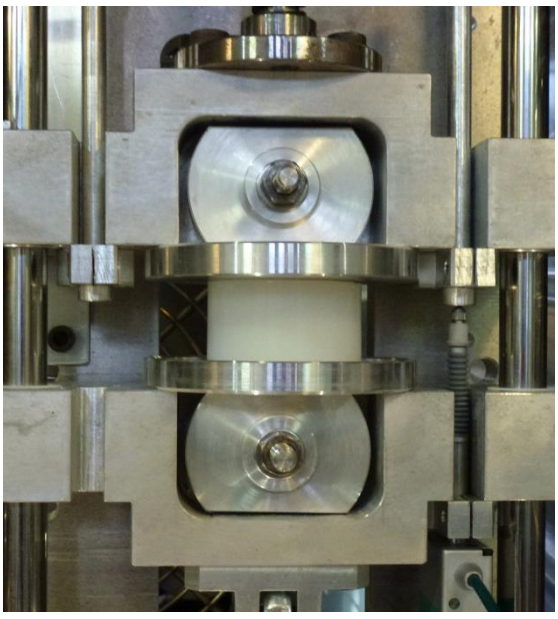

Figure 2: (a) Experimental apparatus designed and realised at INRiM to perform uniaxial unconfined compression. (b) Detail of the experimental apparatus during a sample compression.

Compressive testing requires that TMMs have flat and parallel surfaces, characteristics that are guaranteed by the shape of the mould used for the gel casting. The mould consists of a Plexiglas cylinder furnished of two smooth caps in Teflon. Moreover, the presence of a lateral hole on the cylinder surface lets the air to come out, preventing its entanglement inside the phantom during the sample jellification.

Once cooled, TMM samples thickness is measured by means of a height gauge joined to a feeler pin, whose resolution is ± 0.01 mm and the accuracy is ± 0.03 mm, while gels diameter is measured using a digital calliper with a resolution of ± 0.01 mm. Sample dimensions are measured at the laboratory temperature of about $T = (23.0 \pm 0.5)$ °C and ambient pressure.

During the experiment, both the experimental apparatus and samples have been placed in a temperature chamber to guarantee the temperature stability during the measurement and to have the possibility to change T value during the test. The temperature of the sample under test has been monitored by means of a platinum resistance thermometer (PRT) placed inside a twin gel of that one investigated and positioned in the same chamber.

Since hydrogels can be subject to relevant degradation if not preserved in a controlled environment, during the experiment TMMs have been stored in a sealed and isolating membrane to avoid water evaporation and to maintain constant their humidity. Indeed, with the increase of the temperature during the experiment, changes in the hydrogel structure can occur because of water loss. As a consequence, variations in elastic modulus values associated to the result of the water loss rather than to the properties of the sample of interest [13] could be observed.

3 Results and Discussion

3.1 Fundamental mechanical behaviour

The mechanical behaviour of TMMs have been firstly investigated in compression until failure on the basis of stress-strain measurement in order to define their elastic region below the value of the

yield strength, $_y$, and to define the tensile strength, $_T$, to which yield strain, $_y$ and tensile strain, $_T$, values correspond.

Samples have been placed between two aluminium parallels plates and have been compressed by a linear displacement acting perpendicularly on the upper surface of gels. Parallel plates have been lubricated with a thin layer of glycerine in order to prevent any friction between samples and plates and also to guarantee a homogeneous uniaxial deformation. The effect of lateral expansion during compression, in terms of surface area variation dA (at boundary, dA/dt = 0), has been taken into account in order to achieve directly the stress-strain curve as a function of the actual surface area expansion, A+dA, due to the lateral Poissonian deformation. Surface area variation dA has been determined evaluating the difference between the surface area at a 0 and at 0.10 strain rate value. The dA measurement uncertainty ranges between 0.7% and 1%.

Measurements have been carried out at the constant temperature of 20 °C and at a constant strain rate of $0.1 \cdot 10^{-2}$ s^{-1}. Initially, all investigated samples have a cylindrical shape with thickness, l_0, radius, r, and density, values as reported in Table 2.

	l_0 / mm	$u(l_0)$/ mm	r / mm	$u(r)$ / mm	/ kg·m^{-3}	$u(\ )$ kg·m^{-3}
TMM 1	29.99	0.05	25.08	0.26	1026	21
TMM 2	30.16	0.05	25.08	0.26	984	21
TMM 3	30.23	0.05	25.08	0.26	1045	22
TMM 4	29.79	0.05	25.08	0.26	1034	22
TMM 5	30.12	0.05	25.08	0.26	1030	22
TMM 6	30.16	0.05	25.08	0.26	1043	22
TMM 7	30.18	0.05	25.08	0.26	1027	21
TMM 8	30.17	0.05	25.08	0.26	1049	22
TMM 9	30.03	0.05	25.08	0.26	1076	23

Table 2: Thickness, l_0, radius, r, and density, of investigated tissue mimicking materials with respective uncertainties.

TMM sample stress-strain curves obtained from the compressive tests are shown in Figures 3. To compare samples properties, stress-strain curves have been divided in four different groups. In Figure 3a, TMM 1 and TMM 2, both samples without scattering agents, are represented to show

differences between a simple Agar based tissue-mimicking material, largely studied from a mechanical and thermal point of view, and a Gellan Gum based TMM. On the contrary in panel b, c and d of the same figure, TMM 2 has been compared to TMMs with scattering agents, respectively only kieselghur (panel b), only SiC (panel c) and both kieselghur and SiC in different concentrations (panel d). For each sample, values of $_y$, $_y$, $_T$ and $_T$ are reported in Table 3.

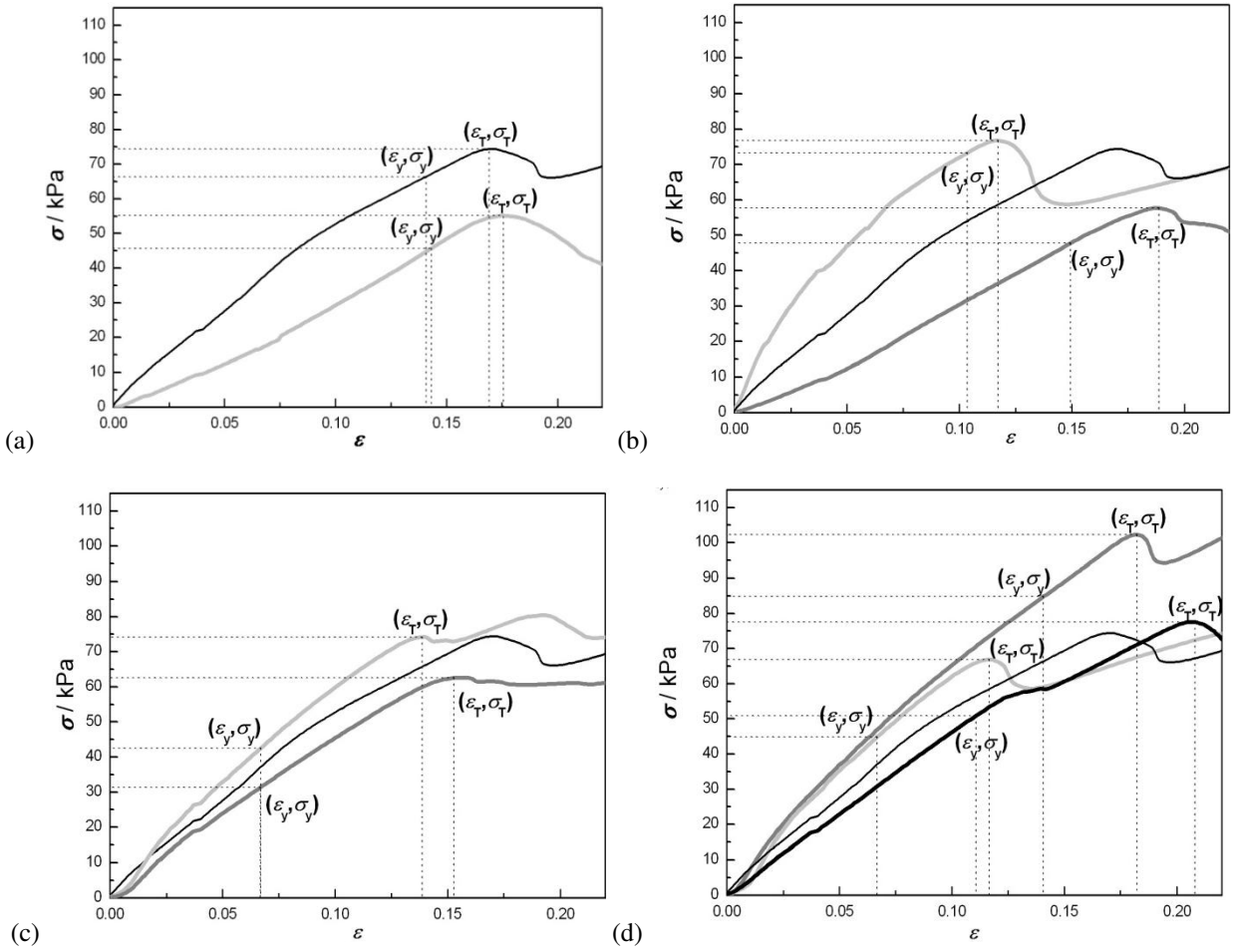

Figure 3: Stress – strain curves in compression test until failure with the indication of $_y$, $_y$, $_T$ and $_T$ values of the nine tested hydrogels. (a) TMM 1, TMM 2; (b) TMM 4, TMM 3, TMM 2; (c) TMM 6, TMM 5, TMM 2; (d) TMM 9, TMM 8, TMM 7, TMM 2.

	$_y$ / kPa	$_y$ / %	$_T$ / kPa	$_T$ / %
TMM 1	45.69	14.32	55.13	17.57
TMM 2	66.43	14.08	74.39	16.91
TMM 3	73.31	10.35	76.78	11.72
TMM 4	47.74	14.95	57.66	18.85
TMM 5	42.52	6.71	74.20	13.87

TMM 6	31.33	6.68	62.54	15.28
TMM 7	44.91	6.67	66.89	11.67
TMM 8	84.75	14.08	102.28	18.24
TMM 9	50.89	11.07	77.54	20.79

Table 3: Tissue-mimicking mechanical properties where $_y$ and $_T$ are respectively the yield and tensile strengths, while $_y$ and $_T$ are respectively the yield and tensile strains.

The yield strength point, $_y$, represents the limit of the sample elastic region, that means that, within the correspondent strain range, the sample shows an elastic behaviour. Maintaining opportunely below $_y$, it is possible to prevent any permanent deformation in the samples during experimental tests. For each sample, the yield strength point has been determined calculating the polynomial curve that better approximates the experimental points of the stress-strain curve and studying the second derivative behaviour. The yield strain represents the value for which the second derivative nullifies.

3.2 Temperature and strain-rate effects

Within the elastic region, the Young's modulus of twin TMMs samples has been determined both as a function of temperature (T varying between 20 °C and 35 °C) and as a function of strain-rate ($\dot{\varepsilon}$ varying between $0.06 \cdot 10^{-2}$ s^{-1} and $0.4 \cdot 10^{-2}$ s^{-1}).

Measurements have been performed in a temperature chamber whose temperature stability is ± 0.5 °C. The whole measuring device has been placed inside the chamber in order to keep both materials under test and instrumentation in thermal equilibrium. In the considered range of temperature, the thermal effects do not affect the effectiveness of the linear encoder and the load cell. Moreover, consequences due to the thermal dilatation of the measuring system can be considered as irrelevant respect to displacements under investigation. Measurements have been carried out at steps of 5 °C and samples have been compressed at four different constant strain-rate

values included between $0.06 \cdot 10^{-2}$ s^{-1} and $0.4 \cdot 10^{-2}$ s^{-1}, approximately doubling the speed of the rate at each step.

Before starting measurements, TMMs, sealed by means of an isolating membrane, have been conditioned for six hours in the temperature chamber at the *T* value chosen for the test.

Considering Eq.(1), the quantity *E* has been determined applying a linear fit to the measured stress-strain curve in the previously defined elastic region. The line angular coefficient supplies the Young's modulus value.

Figures 4 and 5 show values of elastic moduli resulting from compression measurements carried out at different temperatures and strain-rate for TMM 1, taken as an example since its well-known properties.

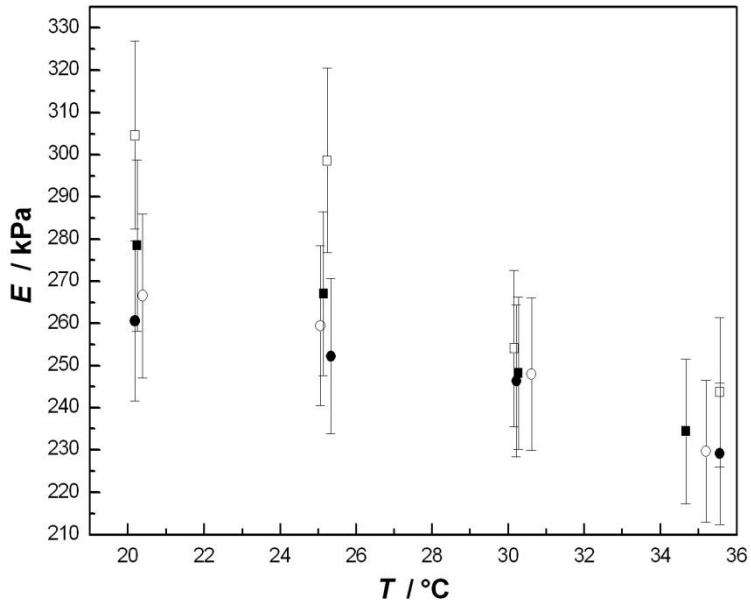

Figure 4: Young's modulus, *E*, and corresponding uncertainty as a function of the temperature, *T*, for TMM 1.
● $\dot{\varepsilon}$ = $0.06 \cdot 10^{-2}$ s^{-1}; ○ $\dot{\varepsilon}$ = $0.1 \cdot 10^{-2}$ s^{-1}; ■ $\dot{\varepsilon}$ = $0.23 \cdot 10^{-2}$ s^{-1}; □ $\dot{\varepsilon}$ = $0.4 \cdot 10^{-2}$ s^{-1}.

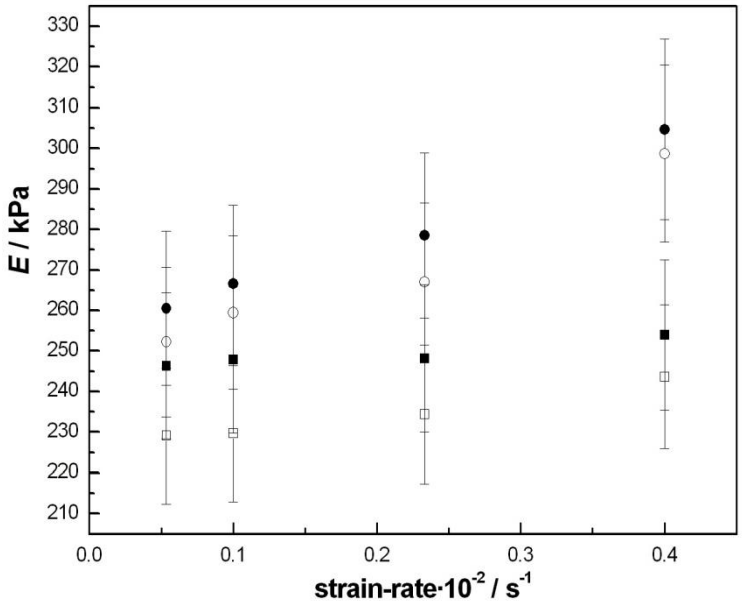

Figure 5: Young's modulus, E, and corresponding uncertainty as a function of the strain-rate, $\dot{\varepsilon}$, for TMM 1. ● T = 20 °C; ○ T = 25 °C; ■ T = 30 °C; □ T = 35 °C.

The uncertainty bars associated to E values have been obtained combining contributions listed in Table 4 and applying the uncertainty propagation to Eq.(1).

Quantity	Relative uncertainty
Force, F	0.2%
Area, A	2.1%
Lateral expansion, dA	1.0%
Thickness, l_0	0.2%
Thickness displacement, l_0	0.2%
Fit parameter	3.4%
Selection of measurement region	6.1%
Overall Young's modulus uncertainty	7.4%

Table 4: Uncertainty budget for the Young's modulus measurement

As it is possible to notice from Table 4, the main part of the uncertainty balance is given by the choice of the measurement region considered for the linear fit. Within the elastic region, varying the range in which the curve is fitted, a relative uncertainty of about 6% is introduced on the E quantity. Repeatability has been evaluated by measuring both Young's modulus and yield strength on 3 different samples of Agarose (TMM 1) and 3 different samples of Phytagel (TMM 2).

Obtained values are consistent within the overall Young's modulus uncertainty. Repeatability strongly depends on TMMs realization and conservation. Inaccurate preparation involves, as an example, differences in shape and/or presence of bubbles in the bulk; inaccurate conservation involves degradation due to water loss.

As observed from experimental data, stiffness varies, with a linear behaviour, as a function of the temperature, T, and with a logarithmic behaviour, as a function of the strain-rate, $\dot{\varepsilon}$.

In order to gather the temperature and strain-rate dependence of Young's modulus, a 3D-graph from experimental data has been generated, as shown in Figure 6. The following representation allows to clearly identify the whole Young's modulus average variability in the considered ranges of temperature and strain-rate. The grey surface area, i.e. $E(T, \dot{\varepsilon})$, is obtained from the best fit of experimental data, on the basis of a constitutive model, as explained in the following section.

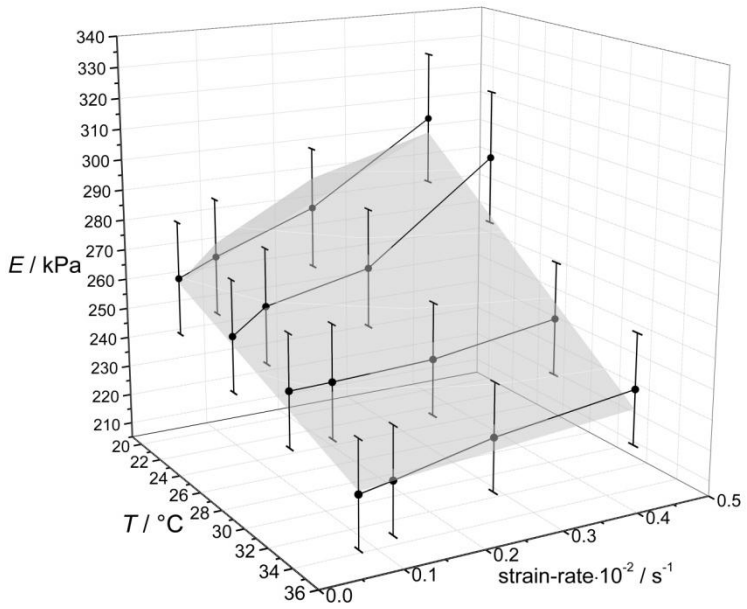

Figure 6: 3D-graph of the Young's modulus, E, and corresponding uncertainty as a function of temperature, T, and strain-rate, $\dot{\varepsilon}$, for TMM 1.

3.3 The Young's modulus constitutive model

Hydrogels properties are dependent on both temperature and strain-rate and it is useful to curve-fit the whole range of test results to a single equation, that is temperature and strain-rate dependent. So using experimental data, a statistical method incorporating multiple linear regression has been employed to identify the temperature and strain-rate dependent mechanical properties of tested hydrogel samples. The combined effects of temperature and strain-rate on E can be determined on the basis of the following constitutive model [32]:

$$E(T,\dot{\varepsilon}) = (a_0 + a_1 T) + (a_2 + a_3 T) \times \ln(\dot{\varepsilon}), \qquad (3)$$

where $\dot{\varepsilon}$ is the strain-rate, T is the temperature, a_0, a_1, a_2, and a_3 are constants depending on the material properties. Introducing two temperature dependent parameters $(T) = (a_0 + a_1 T)$ and $(T) = (a_2 + a_3 T)$, equation (3) can be simplified as:

$$E(T,\dot{\varepsilon}) = \alpha(T) + \beta(T) \times \ln(\dot{\varepsilon}). \qquad (4)$$

Relations (3) and (4) allow to evaluate the combined variation of the Young's modulus as a function of temperature and strain-rate, as depicted in the following graphs. The Young's modulus dependence is represented as a surface in the area defined by experimental data, as shown in the Figure 7.

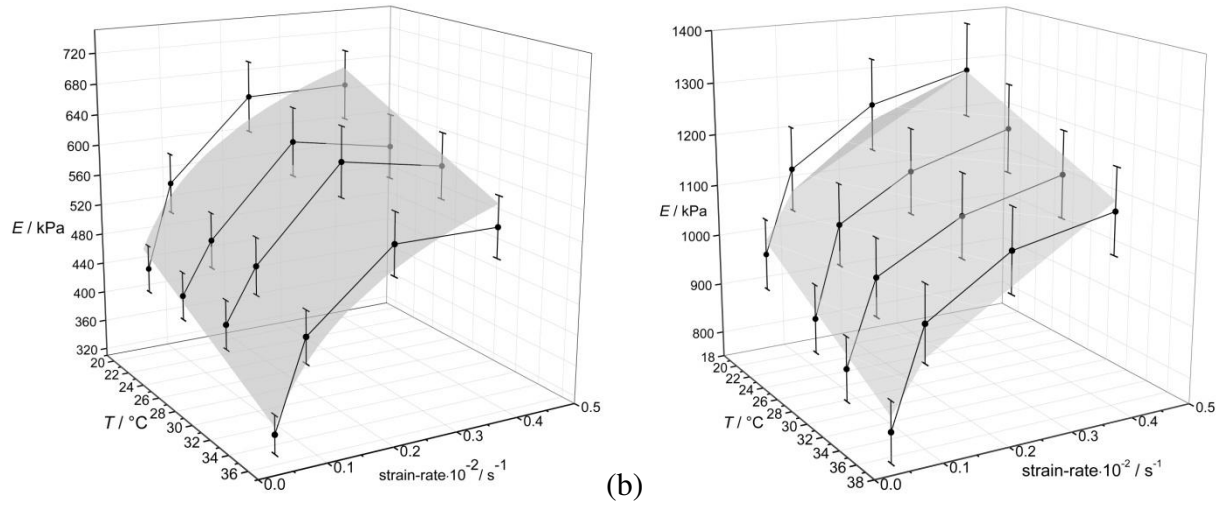

(a) (b)

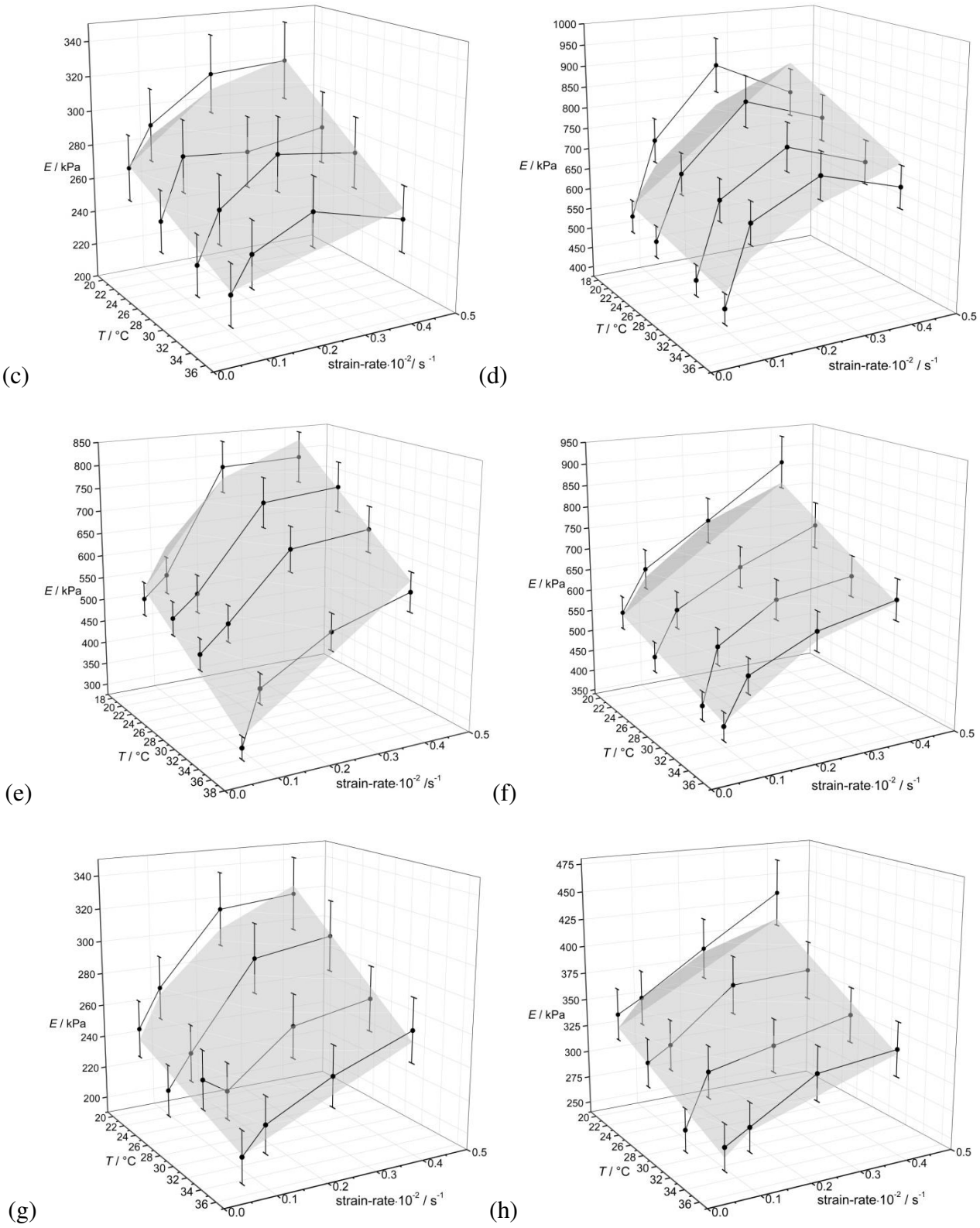

Figure 7: 3D-graph of the Young's modulus, E, and corresponding uncertainty as a function of temperature, T, and strain-rate, $\dot{\varepsilon}$, for (a) TMM 2, (b) TMM 3, (c) TMM 4, (d) TMM 5, (e) TMM 6, (f) TMM 7, (g) TMM 8, (h) TMM 9.

As the strain-rate increases and temperature decreases, viscoelastic materials tend to become more brittle, being the most apparent result an increase in yield stress. As an example, the stress–strain curves of alginate hydrogels [33] are highly dependent on the strain-rate and exhibit a nonlinear behaviour, which is also observed in tensile tests of tendons and ligaments [34, 35]. Even for very low strain-rate values, a relevant increase in hydrogel TMMs Young's modulus is observed, as in other typology of polymers [36] occurs.

In Table 5, fitting parameters and related uncertainties are shown.

Samples	a_0 kPa	$u(a_0)$ kPa	a_1 kPa·°C^{-1}	$u(a_1)$ kPa·°C^{-1}	a_2 kPa	$u(a_2)$ kPa	a_3 kPa·°C^{-1}	$u(a_3)$ kPa·°C^{-1}
TMM 1	470	39	-6	1	42	12	-1.1	0.4
TMM 2	1033	196	-7	7	102	57	0.3	1.9
TMM 3	1747	207	-7	7	129	62	0.9	2.1
TMM 4	495	51	-6	2	43	16	-0.8	0.5
TMM 5	1512	348	-15	12	208	101	-2.7	3.5
TMM 6	1465	210	-17	7	171	60	-1.4	2.0
TMM 7	1522	149	-19	5	209	43	-3.2	1.5
TMM 8	569	58	-8	2	71	17	-1.4	0.6
TMM 9	652	71	-7	3	64	21	-1.0	0.7

Table 5: Parameters values and respective uncertainties obtained from fitting procedure of experimental data with Eq.(3).

Using the proposed constitutive model, it is possible to quantify the magnitude of the average variation of the tested TMMs mechanical behaviour as a function of temperature and strain-rate.

Moreover, it is possible to extend the surface values beyond the experimental data, in order to estimate the mechanical behaviour of tested TMMs, for lower or higher values of temperature and strain-rate. Nevertheless, the estimated values must be considered within probabilistic uncertainties increasing with arithmetical progression for T and geometrical progression for $\dot{\varepsilon}$.

3.4 Relaxation time

Relaxation time, joined to stress, strain and elastic moduli, allows to implement several classic models from which viscoelastic properties of materials can be gather from. The slope of the stress relaxation curve (see Fig. 8) is fitted by using the Kohlrausch-Williams-Watts (KWW) [37, 38] time decay function (Eq. 2).

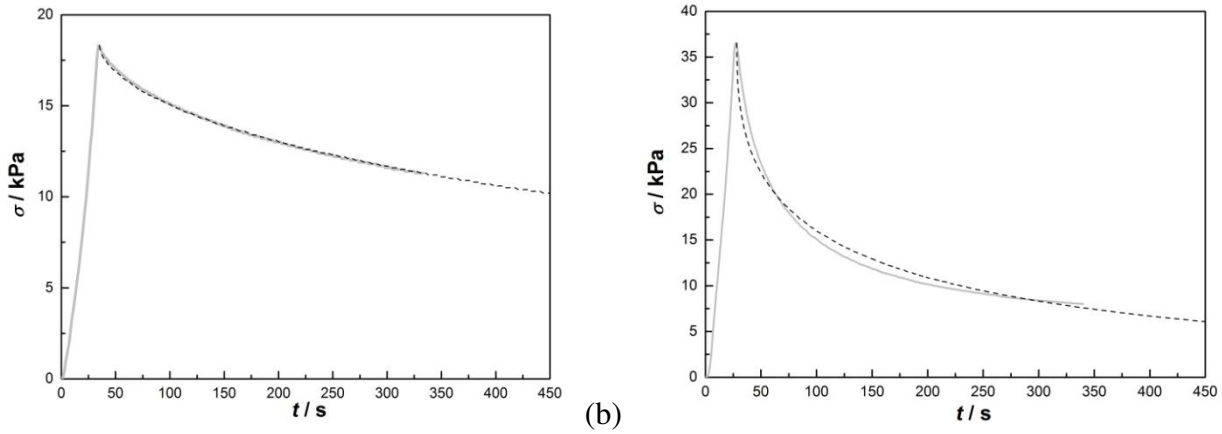

Figure 8: Relaxation experimental curve (grey) and fitting KWW time decay function (dotted line) at T = 30 °C and $\dot{\varepsilon}$ = 0.06·10^{-2} s^{-1} for (a) TMM 1 and (b) TMM 2.

This function establishes a relation between the relaxation time and the molecular behaviour of a material. Indeed, the -term in the KWW stretched-exponential characterizes the degree of non-exponentiality of the relaxation function and, physically, it describes the extent of the molecular coupling within a polymer [39, 40]. The -term can be associated with a coupling parameter, n = 1- , describing the degree of intermolecular cooperativity [41]. For TMMs studied in this work, $_0$ and values resulting from the KWW non-linear fitting analysis are reported in Table 7 as a function of strain-rate and temperature.

	$_0$ / s								±	( )
$\dot{\varepsilon}$ / s^{-1}	0.06·10^{-2}				0.23·10^{-2}					
T / °C	20	25	30	35	20	25	30	35		
TMM 1	1600	1250	1020	(1400)	1080	930	800	740	0.61	0.05
TMM 2	470	360	280	230	490	420	300	250	0.50	0.08
TMM 3	310	260	180	150	350	290	180	140	0.42	0.02
TMM 4	880	880	820	770	900	840	730	720	0.63	0.06
TMM 5	430	380	300	260	480	440	350	300	0.53	0.04
TMM 6	780	650	540	460	(500)	620	540	520	0.54	0.04
TMM 7	440	380	350	320	520	430	360	340	0.53	0.03
TMM 8	1000	1100	1000	800	1150	1200	1100	800	0.73	0.05
TMM 9	580	540	460	400	620	500	470	440	0.51	0.01

Table 5: Values of relaxation time, $_0$, and term as a function of the strain-rate, $\dot{\varepsilon}$, and the temperature, *T*, for all samples investigated.

As it is possible to notice from experimental data analysis, in Phytagel samples the presence of different quantity and kind of solid particles allows to modify the stress relaxation time $_0$, therefore the whole viscoelastic behaviour of samples. Stress relaxation time greatly decreases as temperature increases, while it seems to be less sensitive with respect to strain-rate effects. In general terms, the observed results suggest that samples tend to become more dampened increasing *T* toward human body typical temperature (37 °C).

On the other hand, since values of exponent varies between 0.7 and 0.4, a non-linear viscoelastic behaviour can be recognized (where for classical linear viscoelastic behaviour is intended Maxwell or Voigt models), as actually excepted in polymers [42].

3.5 Microscopy and microanalysis characterization

The results obtained from mechanical tests have highlighted the need of further investigations in order to explain the remarkable difference of $_y$ and $_T$ observed for samples containing SiC and/or kieselguhr. Thus, a microscopic analysis has been performed on a sample containing both particles, specifically on sample classified as TMM 8. Microanalysis and secondary electrons SEM imaging have been performed with a FEI Inspect-F SEM-FEG equipped with EDAX, while low-vacuum SEM imaging has been performed with the dual-beam FEI Quanta 3D-FEG.

As it is possible to observe in Figure 9, which shows a SEM image of a slice of TMM 8, the solid particles are well evident on the polymer matrix surface. It is worth to note that the kieselguhr particles (round drilled cylinders) appear still embedded under the surface and, owing to their shape, surrounded and filled by the polymer matrix. On the contrary, SiC particles do not have a uniform and characteristic shape and appear more as solid small bits dispersed on polymeric matrix surface.

Although this image shows only a small fraction of the sample, a speculation about these particles effects on $_y$ and $_T$ values can be assumed. Comparing $_y$ values between TMM 3 and TMM 4 and between TMM 5 and TMM 6, it appears evident the presence of a "saturation" effect on the increase of gel strength associated to solid particles presence. This phenomenon, also observed in polymers filled with nanocomposites [36], might be due to the presence of micro-defects and/or the formation of low-tensile cracking edges inside the sample. As the concentration of solid particle increases beyond a threshold, a reduction of gel strength is observed. Moreover, comparing TMM 5 to TMM 3, it is evident that the presence of kieselguhr enhances $_y$ value. In this case, the effect could be ascribed to the different shape of these filling particles. Cylindrical hollow shape of kieselguhr lets it to be easily surrounded and filled by the polymer, while its drilled shape creates a sort of micro-grids which give to the sample a greater resistance to mechanical stress respect to when only SiC particles are present. This softening effect is also evident by comparing different relaxation times (see table 5), which appear longer for samples TMM 4 and TMM 6 than for samples TMM 3 and TMM 5 respectively. The temperature dependence of relaxation time is greater for samples with a lower value of (see for example value for samples TMM 4 and TMM 6), that should mean a greater intermolecular cooperativity of the polymer [35 - 36]. The value of TMM 4 lets to suppose that micro-grids given by kieselguhr mostly reduce the elastic response of the polymer matrix. However, results obtained for TMM 7, 8, 9 reveal that the behaviour of samples filled with both particles is less predictable. In this case, a "saturation" effect on the yield strengths is evident (see table 3), but the relaxation time data show that a sort of "competitive" effect between the two filling particles occurs. Indeed, yield strengths of TMM 7 and TMM 9 samples result similar to that one of TMM 4 or TMM 5, as if the effects caused by the presence of SiC were predominant; on the contrary, sample TMM 8 shows the greater value of $_y$ but also the longer relaxation time and the greater value of . Our hypothesis is that, for this particular

concentration value, the kieselguhr effects are predominant, while for lower and greater concentration the defects formation, given by the presence of SiC, hides the hardening effect of kieselghur. Of course this hypothesis should be confirmed by further investigations, varying each particles concentration respect to the others, while in this case we chose to maintain constant the ratio of the two filling particles, evidencing their role on modifying and tuning mechanical properties of tissue mimicking polysaccharide for scaffold and biomedical applications.

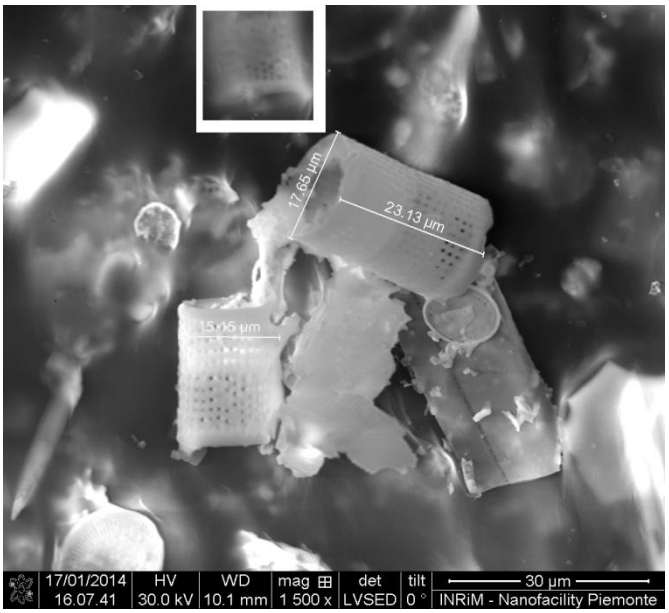

Figure 9: SEM image of TMM 8. Kieselghur cylindrical particles are well visible. On the top (white square) a Kieselghur particle surrounded by the polymer matrix is evidenced.

4 Conclusions

Since hydrogels mechanical properties are strictly linked to several biological features, such as biocompatibility and functionality of biomaterials, and, as recently observed, the Young's modulus significantly influences adhesion, growth and differentiation of cells in scaffolds, an accurate characterization of their elastic and viscoelastic behaviour plays a fundamental role in biomedical applications. Moreover, hydrogels are also extensively used in laboratory tests. For instance, they are used as versatile platform in the study of cell-substrate interactions as well as tissue-mimicking

materials (TMMs) in the investigation of mechanical and thermal effects in tissues due to ultrasounds.

As hydrogels show both elastic and viscoelastic behaviour, their mechanical properties are influenced by strain-rate and temperature. In this work the dependence on strain-rate and temperature of the Young's modulus and relaxation time of nine hydrogel samples (Agar and Phytagel based) has been quantified on the basis of accurate experimental data. Limited to this case study, a constitutive model of Young's modulus, as a function of temperature and strain-rate, have been also defined, in order to highlight the magnitude of mechanical properties fluctuations. Moreover, the presence of solid particles into the hydrogel matrix has been observed to greatly modify mechanical properties of the materials, revealing that a simple preparation procedure can change its elastic properties according to its purpose.

Acknowledgements

The research leading to these results is conducted in the frame of the EMRP JRP HLT03 and partially in the frame of EMRP JRP IND05. The EMRP is jointly funded by the EMRP participating countries within EURAMET and the European Union. This work has been partially performed at NanoFacility Piemonte, INRiM, a laboratory supported by Compagnia di San Paolo.

References

[1] Nayar V.T., Weiland J.D., Nelson C.S., Hodge A.M., J. Mech. Behav. Biomed., *Elastic and viscoelastic characterization of agar*, 2011, 7:60 – 68.

[2] Franke O., Göken M., Hodge A.M., JOM, *The nanoindentation of soft tissue: current and developing approaches*, 2008, 60:49–53.

[3] Nayar V.T., Weiland J.D., Hodge A.M., Mater. Sci. Eng., C, *Characterization of porcine sclera using instrumented nanoindentation*, 2011, 31:796–800.

[4] Ebenstein D.M., Pruitt L.A., J. Biomed. Mater. Res. Part A, *Nanoindentation of soft hydrated materials for application to vascular tissues*, 2004, 69A:197–372.

[5] Basinger B.C., Rowley A.P., Chen K., Humayun M.S., Weiland J.D., J. Neural. Eng., *Finite element modeling of retinal prosthesis mechanics*, 2009, 6(5):055006.

[6] Colodetti L., Weiland J.D., Colodetti A., Ray A., Seiler M.J., Hinton D.R., Humayun M.S., Exp. Eye. Res., *Pathology of damaging electrical stimulation in the retina*, 2007, 85:23–33.

[7] Franke O., Durst K., Maier V., Göken M., Birkholz T., Schneider H., Hennig F., Gelse K., Acta Biomater., *Mechanical properties of hyaline and repair cartilage studied by nanoindentation*, 2007, 3:873–881.

[8] Verma V., Verman P., Kar S., Ray P., Ray A.R., Biotechnol. Bioeng., *Fabrication of agar-gelatin hybrid scaffolds using a novel entrapment method for in vitro tissue engineering applications*, 2006, 96:392–400.

[9] Dave P.C., Dingal P., Discher D.E., Curr. Opin. Biotechnol., *Material control of stem cell differentiation: challenges in nano-characterization*, 2014, 28:46–50.

[10] Lafon C., Zderic V., Noble M.L., Yuen J.C., Kaczkowski P.J., Sapozhnikov O.A., Chavrier F., Crum L.A., Vaezy S., Ultrasound Med. Biol., *Gel phantom for use in high-intensity focused ultrasound dosimetry*, 2005, 31:1383-1389.

[11] O'Neill T.P., Winkler A.J., Wu J., Ultrasound Med.Biol., *Ultrasound heating in a tissue-bone phantom*, 1994, 20(6):579-588.

[12] Arvanitis C.D., McDannold N., Med. Phys., *Integrated ultrasound and magnetic resonance imaging for simultaneous temperature and cavitation monitoring during focused ultrasound therapies*, 2013, 40(11):112901.

[13] Anseth K.S., Bowman C.N., Brannon-Peppas L., Biomaterials, *Mechanical properties of hydrogels and their experimental determination*, 1996, 17:1647-1657.

[14] Snedeker J.G., Niederer P., Schmidlin F.R., Farshad M., Demetropoulos C.K., Lee J.B., Yang K.H., J. Biomech., *Strain-rate dependent material properties of the porcine and human kidney capsule*, 2005, 38(5):1011–1021.

[15] Zioupos P., Hansen U., Currey J.D., J. Biomech, *Microcracking damage and the fracture process in relation to strain rate in human cortical bone tensile failure*, 2008, 41(14): 2932-2939.

[16] Hansen U., Zioupos P., Simpson R., Currey J.D., Hynd D., J. Biomech. Eng., *The effect of strain rate on the mechanical properties of human cortical bone*, 2008, 130(1): 011011.

[17] Huang J., Holt R.G., Cleveland R.O., Roy R.A., J. Acoust. Soc. Am., *Experimental validation of a tractable numerical model for focused ultrasound heating in flow-through tissue phantoms*, 2004, 116(4): 2451-2458.

[18] Culjat M.O., Goldenberg D., Tewari P., Singh R.S., Ultrasound Med Biol., *A review of tissue substitutes for ultrasound imaging*, 2010, 36(6): 861-873.

[19] IEC 61685:2002, *Ultrasonics - Flow measurement systems - Flow test object* (Geneva: International Electrotechnical Commission). BS EN 61685:2002, IEC 61685:2001.

[20] Zohora F.T., Azim A.Y.M.A., *Biomaterials as porous scaffolds for tissue engineering applications: a review*, European Scientific Journal, 2014, 10(21): 1857 - 7431.

[21] Gong Y., Wang C., Lai R.C., Su K., Zhang F., Wang D., J. Mater. Chem., *An improved injectable polysaccharide hydrogel: modified gellan gum for long-term cartilage regeneration in vitro*, 2009, 19:1968–1977.

[22] Morris E.R., Nishinari K., Rinaudo M., Food Hydrocolloid, *Gelation of gellan – A review*, 2012, 28(2):373–411.

[23] CP Kelco Product Infromtation: KELCOGEL, gellan gum, 2007.

[24] Kirchmajer D.M., Steinhoff B., Warren H., Clark R., in het Panhuis M., Carbohydr. Res., *Enhanced gelation properties of purified gellan gum*, 2014, 388 (1), 125-129.

[25] Saddow S.E., *Silicon Carbide Biotechnology. A Biocompatible Semiconductor for Advanced Biomedical Devices and Applications*, 2012, Elsevier (USA), ISBN: 978-0-12-385906-8.

[26] Gnanamoorthy P., Anandhan S., Ashok Prabu V., J. Porous Mater., *Natural nanoporous silica frustules from marine diatom as a biocarrier for drug delivery*, 2014 , 21:789–796.

[27] López-Alvarez M., Solla E.L., González P., Serra J., León B., Marques A.P., Reis R.L., J. Mater. Sci. Mater. Med., *Silicon-hydroxyapatite bioactive coatings (Si-HA) from diatomaceous earth and silica. Study of adhesion and proliferation of osteoblast-like cells*, 2009, 20(5):1131-1136.

[28] Cuccaro R., Musacchio C., Giuliano Albo P.A., Troia A., Lago S., Ultrasonics, *Acoustical characterization of polysaccharide polymers tissue-mimicking materials*, 2015, 56:210-219.

[29] Anderssen R.S., Husain S.A., Loy R.J., Anziam J., *The Kohlrausch function: properties and applications*, 2004, 45: C800–C816.

[30] ISO 376:2011, *Standard for calibrating force transducers*.

[31] ISO 5893:2002, *Rubber and plastics test equipment - Tensile, flexural and compression types (constant rate of traverse) – Specification*.

[32] Shi X.Q., Zhou W., Pang H.L.J., Wang Z.P., J. Electron. Packag., *Effect of Temperature and Strain Rate on Mechanical Properties of 63Sn/37Pb Solder Alloy*, 1999, 121(3):179-185.

[33] Drury J.L., Dennis R.G., Mooney D.J., Biomaterials, *The tensile properties of alginate hydrogels*, 2004, 25:3187–3199.

[34] Woo S.L.Y., Young E.P., *Structure and function of tendons and ligaments,* in: V.C. Mow, W.C. Hayes (Eds.), Basic orthopaedic biomechanics, 1991, New York: Raven Press Ltd, pp. 199 –243.

[35] Park J.B., Lakes R.S., *Structure-property relationships of biological materials*, in J.Y. Wong, J.D. Bronzino (Eds.), Biomaterials: an introduction, 2nd ed., 2001, New York: Plenum Press, pp. 185–222.

[36] Zhou Y., Mallick P.K., Polym. Eng. Sci., *Effects of temperature and strain rate on the tensile behavior of unfilled and talc-filled polypropylene. Part I: experiments*, 2002, 42(72):2449-2460.

[37] Matsuoka S., *Relaxation phenomena in polymers*, 1986, Oxford University Press, New York.

[38] Fancey K.S., J.Mater. Sci., *A mechanical model for creep, recovery and stress relaxation in polymeric materials*, 2005, 40 (18): 4827-4831.

[39] Ngai K.L., Roland C.M., Macromolecules, *Chemical Structure and Intermolecular Cooperativity: Dielectric Relaxation Results*, 1993, 26:6824-6830.

[40] Jancar J., Hoy R.S., Lesser A.J., Jancarova E., Zidek J., Macromolecules, *Effect of particle size, temperature and deformation rate on the plastic flow and strain hardening response of PMMA composites*, 2013, 46:9409–9426.

[41] Ngai K.L., Roland C.M., Macromolecules, *Intermolecular Cooperativity and the Temperature Dependence of Segmental Relaxation in Semicrystalline Polymers*, 1993, 26: 2688-2690.

[42] Roylance D., *Engineering viscoelasticity*, Department of Materials Science and Engineering– Massachusetts Institute of Technology, Cambridge MA, 2001, 2139: 1-37.